Identifying the Tunneling Site in Strong-Field Ionization of H_2^+

Kunlong Liu* and Ingo Barth†
Max-Planck-Institut für Mikrostrukturphysik, Weinberg 2, D-06120 Halle (Saale), Germany
(Received 30 May 2017; revised manuscript received 25 October 2017; published 15 December 2017)

The tunneling site of the electron in a molecule exposed to a strong laser field determines the initial position of the ionizing electron and, as a result, has a large impact on the subsequent ultrafast electron dynamics on the polyatomic Coulomb potential. Here, the tunneling site of the electron of H_2^+ ionized by a strong circularly polarized (CP) laser pulse is studied by numerically solving the time-dependent Schrödinger equation. We show that the electron removed from the down-field site is directly driven away by the CP field and the lateral photoelectron momentum distribution (LPMD) exhibits a Gaussian-like distribution, whereas the corresponding LPMD of the electron removed from the up-field site differs from the Gaussian shape due to the Coulomb focusing and scattering by the down-field core. Our current study presents the direct evidence clarifying a long-standing controversy over the tunneling site in H_2^+ and raises the important role of the tunneling site in strong-field molecular ionization.

DOI: 10.1103/PhysRevLett.119.243204

Tunnel ionization is one of the most fundamental processes in attosecond physics [1,2]. In the picture of tunnel ionization of atoms, the laser field bends the Coulomb potential and the bound electron may tunnel out of the atom through a newly forming barrier. In molecules, however, electrons are bound by Coulomb potentials of several nuclei. Thus, the polyatomic Coulomb potential and the external field can form different barriers for the bound electron localized on different nuclei. It can result in complicated tunneling processes in the three-dimensional space. Even for the simplest molecular system H_2^+, there is still a standing question regarding its tunnel ionization: From which tunneling site in H_2^+ will the electron be removed?

The tunneling site in strong-field ionization indicates the tunnel exit of the electron and there are several tunneling sites in the molecule due to the existence of the polyatomic Coulomb potential [3]. The laser-driven motion of the electron removed from one of different sites is then modified by the polyatomic Coulomb attraction force [4]. Omitting the identification of the tunneling site in theoretical models for molecules may cause deviations between experiments and theoretical predictions. In particular, the strong-field mechanisms of high harmonic generation [5,6], molecular orbital tomography [7,8], photoelectron holography [9,10], and laser-induced electron diffraction [11,12] are sensitive to the electron dynamics after tunneling. For tunnel ionization of molecules itself, the phase structure of the continuum wave packet of the photoelectron is also related to the tunneling site [13,14], which ultimately has the influence on the photoelectron momentum distribution (PMD). Therefore, identifying the tunneling site of the electron is of vital importance for better understanding and finer reconstruction of the ultrafast electron dynamics in molecules. Having such an important role, the tunneling site of the electron is unfortunately often overlooked in many studies of laser-molecular interactions.

A well-known strong-field phenomenon associated with the tunneling site of the electron is enhanced ionization (EI) of molecules [15–22]. It has been shown theoretically [15–18] and experimentally [19–22] that, when the molecule is stretched to a critical internuclear distance, the ionization rate increases significantly. Figure 1 depicts the physical picture explaining the behavior of EI in H_2^+. At the critical internuclear distance, two different barriers are formed by the diatomic Coulomb potential and the external field. Compared to the electron on the down-field site, where a thick outer barrier is formed between the core and the continuum, the up-field electron is much easier to tunnel to the continuum through a thin inner barrier. Within this picture, the molecular ionization from the up-field site is responsible for the enhancement of the ionization.

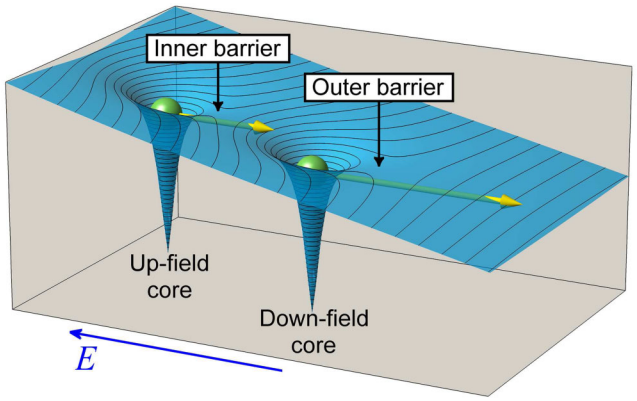

FIG. 1. The tunneling scenario in the field-dressed potential of H_2^+ at the critical internuclear distance. In the presence of the external field, two barriers are formed for the bound electron localized on different nuclei.

To confirm experimentally from which site the electron is preferentially removed, several experiments of molecular ionization have been done by applying two-color fields [23–25] or elliptically polarized pulses [26]. However, their conclusions regarding the tunneling site are contradictory. For EI of H_2^+, which was predicted by theory in the first place, the evidence of the preferential tunneling site is still absent. Although the evolution of the wave function can be simulated in numerical calculations [27,28], it is still difficult to identify from the wave function propagation whether the unidirectional electron transfer from the up-field core to the down-field core is induced by transient electron localization or by direct ionization from the up-field site. Therefore, our challenge is to identify the electron dynamics starting from different tunneling sites using suitable experimental observables.

In this Letter, we show that the preferential tunneling site, which depends on the internuclear distance of H_2^+, can be identified with the lateral photoelectron momentum distribution (LPMD). Our idea is based on the experimentally verified phenomenon that the LPMD for atoms ionized by a circularly polarized (CP) laser pulse is Gaussian [29]. In Fig. 2, we depict the scheme for identifying the tunneling site of the electron in H_2^+ driven by a CP laser pulse. The right CP pulse is polarized in the x-y plane and the molecule is aligned along the x axis. When the rotating electric field vector is parallel to the molecular axis, the ionization rate is expected to be higher [30]. Assuming that the electrons become free at cores 1 and 2 when the rotating electric field vector points at $-\mathbf{e}_x$, the corresponding classical electronic trajectories 1 and 2 driven by the laser field are shown in Fig. 2. Here, trajectories 1 and 2 indicate the paths of the electron removed from the up- and down-field sites, respectively. We can see that the electron along the trajectory 2 is driven away directly, whereas the electron along the trajectory 1 travels through the vicinity of the down-field core. Then, because of the Coulomb interaction with the down-field core, the electron dynamics starting from the up-field site would differ from that starting from the down-field site. In particular, there is no z component of the electric field of the nonrelativistic laser pulse and the Coulomb potential has, thus, the major impact on the lateral electric motion. Therefore, we can identify the tunneling site via the following mechanism: If the electron is removed from the down-field site, the process is similar to the tunneling ionization of atoms by a CP laser pulse, resulting in a Gaussian-like LPMD; in contrast, if the electron is removed from the up-field site, the LPMD will be no longer Gaussian because of the Coulomb effect of the down-field core. The identification is based on whether the lateral electronic motion is strongly affected by another core besides the parent core and, therefore, does not rely on the initial longitudinal momenta of the electron [4]. In addition, by analyzing the LPMD and the corresponding 2D PMDs in the polarization plane, we can reveal further details of the ionization dynamics in H_2^+.

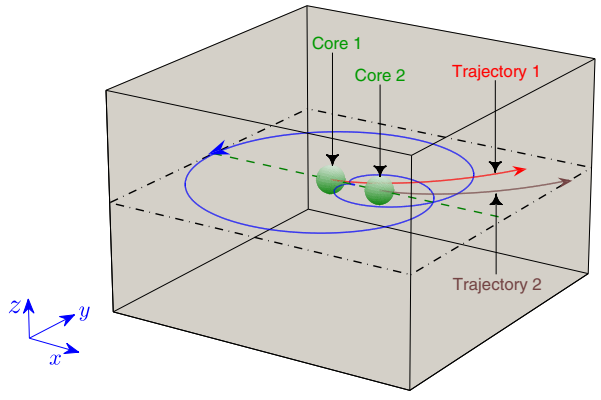

FIG. 2. Scheme for identifying the tunneling site of the electron in the ionization of H_2^+ by a circularly polarized field. The blue curve shows the electric field with the arrow indicating its rotating direction. Trajectories 1 and 2 indicate the classical paths of the freed electron starting at different cores, as described in the text.

Based on the identification scheme above, we study the tunneling site of the electron in H_2^+ via *ab initio* calculations. We solve numerically the three-dimensional (3D) time-dependent Schrödinger equation (TDSE) in Cartesian coordinate system for H_2^+ with fixed internuclear distance R. This molecule is aligned along the x axis and the laser field is polarized in the x-y plane (see Fig. 2). Within the dipole approximation, the length-gauge TDSE is given by (in atomic units)

$$i\frac{\partial}{\partial t}\Psi(\mathbf{r},t)=\left[-\frac{\nabla^2}{2}+V_0(\mathbf{r};R)+\mathbf{r}\cdot\mathbf{E}(t)\right]\Psi(\mathbf{r},t), \quad (1)$$

where $V_0(\mathbf{r};R)=-[|\mathbf{r}-\mathbf{r}_+(R)|]^{-1}-[|\mathbf{r}-\mathbf{r}_-(R)|]^{-1}$ is the Coulomb potential with $\mathbf{r}_\pm(R)=(\pm R/2,0,0)$. The right CP electric field and its vector potential are defined as $\mathbf{E}(t)=-\partial\mathbf{A}(t)/\partial t$ and

$$\mathbf{A}(t)=\frac{\mathcal{E}}{\omega}\cos^4\left(\frac{\omega t}{4}\right)[\sin(\omega t+\phi)\mathbf{e}_x-\cos(\omega t+\phi)\mathbf{e}_y] \quad (2)$$

for $-(2\pi/\omega)<t<(2\pi/\omega)$ with $\mathcal{E}$, ω and ϕ being the field amplitude, the laser frequency, and the carrier-envelope phase (CEP), respectively. For details regarding the numerical method, see Ref. [31].

We calculate the ionization probabilities as a function of the internuclear distance of H_2^+ driven by an 800-nm right CP laser field. The results for $\phi=0$ and different intensities ($I_1=1.25$, $I_2=1.75$, and $I_3=2.25$ in the units of 10^{14} W/cm^2) are shown in Fig. 3(g). We observe two ionization enhancements around $R_1=4.824$ and $R_2=8.040$ a.u. Since the aim of the present work is to identify the tunneling site of the electron when EI takes place, next we will focus on the ionization processes at R_1 and R_2 and also that at $R_0=3.216$ a.u. as a reference.

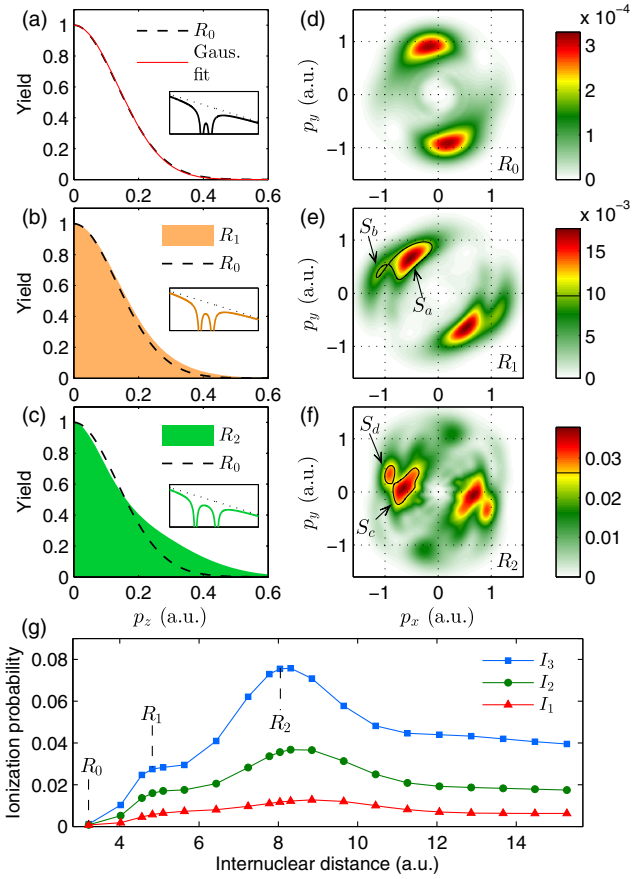

FIG. 3. The CEP-averaged LPMDs (a)–(c) and 2D PMDs (d)–(f) for the ionization of H_2^+ at the internuclear distances R_0, R_1, and R_2 by the 800-nm right CP pulse with the intensity $I_3 = 2.25 \times 10^{14}$ W/cm^2. The shapes of the laser-dressed potentials are illustrated inside (a)–(c). The Gaussian fit for the LPMD for R_0 is also shown in (a). The panel (g) shows the ionization probabilities under the fixed CEP $\phi = 0$ as a function of the internuclear distance.

From TDSE calculations [31], we obtain the CEP-averaged 3D PMDs $Y(p_x, p_y, p_z)$ for R_0, R_1, and R_2 under I_3. The CEP ranges from 0 to 2π with the step of $\pi/18$. We show in Figs. 3(a)–3(c) the LPMDs integrated over p_x and p_y and in Figs. 3(d)–3(f) the 2D PMDs integrated over p_z. Note that all LPMDs are normalized to their maxima and, since the results are averaged over the CEP, the LPMDs are independent on the molecular orientation in the x-y plane. In Fig. 3(a), the LPMD for R_0 fits perfectly to the Gaussian distribution $\exp(-p_z^2/\sigma^2)$ with $\sigma = 0.1933$. For small internuclear distances, the inner barrier is much lower than the outer one. The bound electron would only tunnel through the outer barrier. Thus, the electron after tunneling behaves similarly to that in atomic ionization by a CP laser field, resulting in a Gaussian LPMD [29,32]. The difference is that for H_2^+ the ionization rate is higher when the field vector is parallel to the molecular axis. Therefore, instead of the ring-shaped PMD for the atom, we observe in Fig. 3(d) the distribution with peaks aligned along a certain direction, where the tilted alignment from the y axis is due to the Coulomb effect [30].

Now we turn to the situations for R_1 and R_2, where the inner barriers are comparable with the outer barriers and the electron is localized on the well-separated nuclei. From Fig. 3(b) we can see that the LPMD for R_1 exhibits a similar Gaussian shape compared to that of R_0, indicating that the lateral motion of the photoelectron remains essentially unchanged. The small discrepancy could be due to the different ionization potentials and the weak effect from the diatomic Coulomb potential. In contrast, the LPMD for R_2 shown in Fig. 3(c) is distinct from the Gaussian shape. The distribution is narrowed for low lateral momenta and the enhancement appears for high lateral momenta. The observable change of the LPMD demonstrates that the electron dynamics has been modified by the second core besides of its parent core. Therefore, based on the identification scheme described via Fig. 2, we can conclude from the LPMDs for R_1 and R_2 that, in general, the electron is preferentially removed from the down-field site for R_1 (the first ionization enhancement) but from the up-field site for R_2 (the second ionization enhancement).

To gain more details of the underlying dynamics, we further analyze the LPMDs for R_1 and R_2 by looking into the corresponding 2D PMDs shown in Figs. 3(e) and 3(f). In the 2D PMD for R_1, a small part (indicated by S_b) is divided from the main distribution (indicated by S_a). We extract the LPMDs by integrating the 3D PMD over p_x and p_y near the peaks in the regions of S_a and S_b. The corresponding LPMDs depicted in Figs 4(a) and 4(b) exhibit the closely similar distributions to the Gaussian LPMD for R_0, demonstrating that both parts of the 2D PMD originate from the electron removed from the down-field site. Next, we illustrate in Fig. 4(e) two electronic paths explaining the division of the PMD. The path T_a illustrates the trajectory of the major wave packet tunneling from the down-field site when the field vector is parallel to the molecular axis. This process is responsible for the distribution indicated by S_a in Fig. 3(e). Then, due to the coupling between the ground and the first excited states of H_2^+, the electron from the up-field site could be transiently localized to the down-field core after the field maximum [28,33], leading to another relatively weak ionization burst [3,28], as illustrated by T_b. According to the attoclock configuration [34], the photoelectron from the ionization burst at a delayed time would have a larger offset angle with respect to that of the major ionization. Moreover, compared to T_a, the electron traveling along T_b is closer to the up-field (left) core. Thus, the Coulomb attraction of the up-field core will contribute additionally to the momentum shift to $-\mathbf{e}_x$ and $-\mathbf{e}_y$. As a result, the satellite peaks appear beside the main momentum distribution for R_1.

For the internuclear distance R_2, not only the ionization rate is significantly enhanced, but also the electron

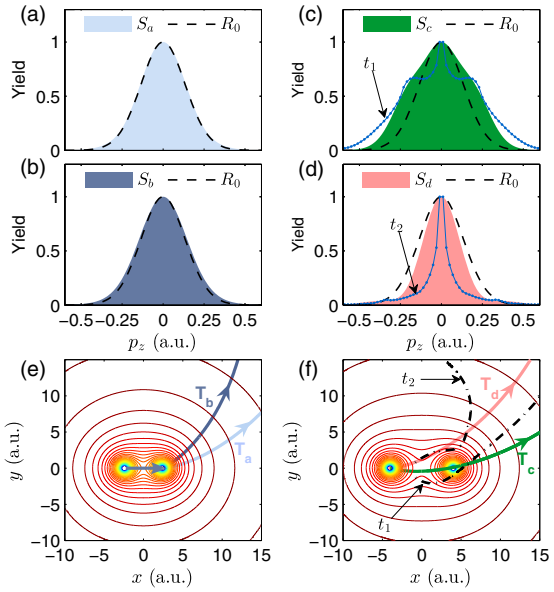

FIG. 4. (a)–(d) The LPMDs for the specific momentum regions indicated in Figs. 3(e) and 3(f), comparing with the Gaussian LPMD for R_0 (dashed curves). Panels (e) and (f) show the Coulomb potentials (contour curves) of H_2^+ at R_1 and R_2 and the paths (thick curves with arrows) illustrating the underlying processes responsible for the corresponding LPMDs. The solid curves with dots in (c) and (d) indicate the LPMDs obtained from semiclassical simulations [35] and the corresponding averaged classical trajectories are depicted by the dash-dotted curves in (f).

dynamics changes essentially, as indicated by the irregular PMDs shown in Figs. 3(c) and 3(f). Similarly, we obtain the LPMDs near the peaks in the distributions circled by S_c and S_d in the 2D PMD for R_2 and the results are shown in Figs. 4(c) and 4(d), respectively. We find that the LPMD for S_c is broader than that for R_0, whereas the LPMD for S_d is narrowed but with a small enhancement for high lateral momenta. Both of the LPMDs demonstrate that the electron motions have been strongly affected by the Coulomb potential after ionization. The underlying mechanisms can be explained by the paths T_c and T_d shown in Fig. 4(f). Along T_c, the electron is removed from the up-field site before $t = 0$ and then is scattered by the down-field core. Because of the strong Coulomb attraction force in the vicinity of the down-field core, the direction of the electronic motion would be deflected, i.e., the zero-lateral-momentum electron could acquire a certain momentum in the lateral direction during the scattering, ultimately resulting in the enhanced distribution for high lateral momenta. For T_d, the electron is removed from the up-field site after $t = 0$ and then travels passing the down-field core. The Coulomb focusing from the down-field core thus gradually reduces the width of the LPMD. A small part of the spreading wave packet for T_d would still be scattered by the down-field core, leading to the weak enhancement for high momenta. To demonstrate the role of the Coulomb focusing and scattering of the down-field core in modifying the

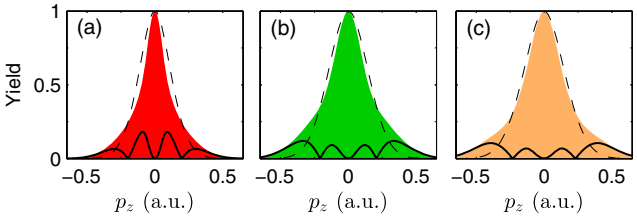

FIG. 5. The LPMDs for R_0 (dashed curves) and R_2 (shadows) and their absolute deviations (solid curves) under three pulse intensities 1.25×10^{14}, 2.25×10^{14}, and 3.25×10^{14} W/cm^2 (from left to right) and $\phi = 0$.

LPMD for R_2, we consider two representative ionization scenarios where the electron is removed from the up-field site at times $t_1 = -12$ and $t_2 = 7.5$ a.u., respectively, and perform the semiclassical simulations [35]. We show the averaged classical trajectories for t_1 and t_2 in Fig. 4(f) and the corresponding LPMDs in Figs. 4(c) and 4(d). The LPMDs obtained from the semiclassical simulations reproduce qualitatively the features (enhancement and narrowed distribution, respectively) of those obtained from TDSE, indicating that the scenarios shown by the averaged classical trajectories in Fig. 4(f) are basically consistent with the underlying mechanisms. Around $p_z = 0$, the LPMDs obtained from TDSE are less cusplike than those from semiclassical calculations. It could be due to the ionization that takes place at the down-field core or at times when the field vector is approximately perpendicular to the molecular axis. We note that the corresponding LPMD (not shown) for the weak signal around $\pm(0.25, 1.10)$ of the 2D PMD in Fig. 3(f) is close to a Gaussian distribution, so the underlying process might be that the electron is transiently localized on the down-field core and then a weak ionization burst occurs at the down-field site.

Furthermore, we show in Fig. 5 the LPMDs for R_0 and R_2 and their absolute deviations under three pulse intensities and $\phi = 0$. For low intensities, the LPMD for R_2 becomes closer to a cusp, because the electron travels relatively slower and the Coulomb focusing by the down-field core reduces the width of the LPMD significantly. For high intensities, the electron is driven away quickly and, therefore, the Coulomb focusing has less significant effect. In this case, the modification of the LPMD at low momenta is less pronounced, but the scattering by the down-field core still leads to the observable enhancement for high lateral momenta.

In conclusion, we have investigated the ionization dynamics of H_2^+ driven by CP laser fields and shown that the interplay between the ionizing electron and the diatomic Coulomb potential depends on the tunneling site of the electron and is ultimately imprinted in the PMD, especially in the LPMD. In particular, we can identify the tunneling site of the electron in H_2^+ with the LPMD. Our identification scheme should be feasible in the few-cycle-pulse pump-probe experiment [22]. Although the identification of the

tunneling site in more general molecules is challenging because the LPMD also depends on the orbital structure [36], we believe the LPMD could be a good entry point for theoretical and experimental studies of molecular ionization. Our results also raises the challenge for theoretical models [14,37–40] to describe the dynamics of the electron through the barriers at different tunneling sites in molecules, where the mechanism is beyond the tunneling picture of atoms, since the ionization rate, the tunnel exit, and the electron motion affected by the polyatomic Coulomb potential after tunneling are all associated with the tunneling site of the electron in the molecule.

We thank M. Lein, N. Eicke, and F. He for helpful discussions. This work was financially supported by the Max Planck Society for the Max Planck Research Group "Current-Carrying Quantum Dynamics" (CCQD).

*klliu@mpi-halle.mpg.de
†barth@mpi-halle.mpg.de

[1] M. Y. Ivanov, M. Spanner, and O. Smirnova, J. Mod. Opt. **52**, 165 (2005).
[2] F. Krausz and M. Ivanov, Rev. Mod. Phys. **81**, 163 (2009).
[3] X. Gong, Q. Song, Q. Ji, H. Pan, J. Ding, J. Wu, and H. Zeng, Phys. Rev. Lett. **112**, 243001 (2014).
[4] J. Wu, M. Meckel, S. Voss, H. Sann, M. Kunitski, L. P. H. Schmidt, A. Czasch, H. Kim, T. Jahnke, and R. Dörner, Phys. Rev. Lett. **108**, 043002 (2012).
[5] J. L. Krause, K. J. Schafer, and K. C. Kulander, Phys. Rev. Lett. **68**, 3535 (1992).
[6] P. B. Corkum, Phys. Rev. Lett. **71**, 1994 (1993).
[7] J. Itatani, J. Levesque, D. Zeidler, H. Niikura, H. Pépin, J. C. Kieffer, P. B. Corkum, and D. M. Villeneuve, Nature (London) **432**, 867 (2004).
[8] C. Zhai, X. Zhu, P. Lan, F. Wang, L. He, W. Shi, Y. Li, M. Li, Q. Zhang, and P. Lu, Phys. Rev. A **95**, 033420 (2017).
[9] Y. Huismans *et al.*, Science **331**, 61 (2011).
[10] Y. Zhou, O. I. Tolstikhin, and T. Morishita, Phys. Rev. Lett. **116**, 173001 (2016).
[11] M. Meckel, D. Comtois, D. Zeidler, A. Staudte, D. Pavičić, H. C. Bandulet, H. Pépin, J. C. Kieffer, R. Dörner, D. M. Villeneuve, and P. B. Corkum, Science **320**, 1478 (2008).
[12] B. Wolter, M. G. Pullen, A.-T. Le, M. Baudisch, K. Doblhoff-Dier, A. Senftleben, M. Hemmer, C. D. Schröter, J. Ullrich, T. Pfeifer, R. Moshammer, S. Gräfe, O. Vendrell, C. D. Lin, and J. Biegert, Science **354**, 308 (2016).
[13] M. Meckel, A. Staudte, S. Patchkovskii, D. M. Villeneuve, P. B. Corkum, R. Dörner, and M. Spanner, Nat. Phys. **10**, 594 (2014).
[14] M. M. Liu, M. Li, C. Wu, Q. Gong, A. Staudte, and Y. Liu, Phys. Rev. Lett. **116**, 163004 (2016).
[15] K. Codling, L. J. Frasinski, and P. A. Hatherly, J. Phys. B **22**, L321 (1989).
[16] K. Codling and L. J. Frasinski, J. Phys. B **26**, 783 (1993).
[17] T. Zuo and A. D. Bandrauk, Phys. Rev. A **52**, R2511 (1995); S. Chelkowski and A. D. Bandrauk, J. Phys. B **28**, L723 (1995).
[18] L. Xin, H. C. Qin, W. Y. Wu, and F. He, Phys. Rev. A **92**, 063803 (2015).
[19] T. Seideman, M. Y. Ivanov, and P. B. Corkum, Phys. Rev. Lett. **75**, 2819 (1995).
[20] E. Constant, H. Stapelfeldt, and P. B. Corkum, Phys. Rev. Lett. **76**, 4140 (1996).
[21] D. Normand and M. Schmidt, Phys. Rev. A **53**, R1958 (1996).
[22] H. Xu, F. He, D. Kielpinski, R. T. Sang, and I. V. Litvinyuk, Sci. Rep. **5**, 13527 (2015).
[23] K. J. Betsch, D. W. Pinkham, and R. R. Jones, Phys. Rev. Lett. **105**, 223002 (2010).
[24] B. Sheehy, B. Walker, and L. F. DiMauro, Phys. Rev. Lett. **74**, 4799 (1995).
[25] M. R. Thompson, M. K. Thomas, P. F. Taday, J. H. Posthumus, A. J. Langley, L. J. Frasinski, and K. Codling, J. Phys. B **30**, 5755 (1997).
[26] J. Wu, M. Meckel, L. Ph. H. Schmidt, M. Kunitski, S. Voss, H. Sann, H. Kim, T. Jahnke, A. Czasch, and R. Dörner, Nat. Commun. **3**, 1113 (2012).
[27] C. Huang, P. Lan, Y. Zhou, Q. Zhang, K. Liu, and P. Lu, Phys. Rev. A **90**, 043420 (2014).
[28] N. Takemoto and A. Becker, Phys. Rev. Lett. **105**, 203004 (2010).
[29] L. Arissian, C. Smeenk, F. Turner, C. Trallero, A. V. Sokolov, D. M. Villeneuve, A. Staudte, and P. B. Corkum, Phys. Rev. Lett. **105**, 133002 (2010).
[30] M. Odenweller, N. Takemoto, A. Vredenborg, K. Cole, K. Pahl, J. Titze, L. P. H. Schmidt, T. Jahnke, R. Dörner, and A. Becker, Phys. Rev. Lett. **107**, 143004 (2011).
[31] K. Liu, K. Renziehausen, and I. Barth, Phys. Rev. A **95**, 063410 (2017); K. Liu and I. Barth, Phys. Rev. A **94**, 043402 (2016).
[32] I. A. Ivanov, Phys. Rev. A **90**, 013418 (2014).
[33] F. He, A. Becker, and U. Thumm, Phys. Rev. Lett. **101**, 213002 (2008).
[34] P. Eckle, M. Smolarski, P. Schlup, J. Biegert, A. Staudte, M. Schöffler, H. G. Muller, R. Dörner, and U. Keller, Nat. Phys. **4**, 565 (2008).
[35] See Supplemental Material at http://link.aps.org/supplemental/10.1103/PhysRevLett.119.243204 for the details of the semiclassical simulations.
[36] I. Petersen, J. Henkel, and M. Lein, Phys. Rev. Lett. **114**, 103004 (2015).
[37] M. Li, J. W. Geng, H. Liu, Y. Deng, C. Wu, L. Y. Peng, Q. Gong, and Y. Liu, Phys. Rev. Lett. **112**, 113002 (2014).
[38] X. Song, C. Liu, Z. Sheng, P. Liu, Z. Chen, W. Yang, S. Hu, C. D. Lin, and J. Chen, Sci. Rep. **6**, 28392 (2016).
[39] N. I. Shvetsov-Shilovski, M. Lein, L. B. Madsen, E. Räsänen, C. Lemell, J. Burgdörfer, D. G. Arbó, and K. Tőkési, Phys. Rev. A **94**, 013415 (2016).
[40] J. Chen, J. Liu, and S. G. Chen, Phys. Rev. A **61**, 033402 (2000).